# Optimization of Flame Stabilization Limits In Meso-Scale Tube Combustors with Wire Mesh

Fudhail Abdul Munir[1], Takehiko Seo[2] & Masato Mikami[2]
[1]Centre for Advanced Research on Energy (CARe), Universiti Teknikal Malaysia Melaka, Malaysia
[2]Graduate School of Science & Engineering, Yamaguchi University Japan

***Abstract*— In the last two decades, with the continued depletion of energy resources and the need for better power sources for small scale devices, researchers have become increasingly interested in meso and micro-scale combustion. Flame stability of a meso-scale combustor depends on a few important factors such as combustor wall thickness, wall thermal conductivity and inner diameter. In order to enhance the combustor performance such as the operational limits, it is vital to fundamentally understand these determinant factors. In this research, simulations and experiments were performed to investigate the factors affecting the flame stabilization in meso-scale tube combustors with stainless steel wire mesh. The inner diameter of the meso-scale cylindrical tube combustors is fixed to 3.5 mm while the wall thickness is maintained at 0.7 mm. The wire mesh is located between the unburned and burned gas region of the combustor. The numerical simulations were performed using a three-dimensional (3-D) numerical model, from which the results in terms of gas and wire mesh temperature contours, blowout limits, combustor outer wall temperature distribution and combustion efficiency were established. In the experiments, the equivalence ratio and mixture flow velocity were varied and the effects in terms of flame stabilization limits were recorded. The main objective of utilizing a 3-D numerical model is to successfully demonstrate the role of thermal path from the tube combustor wall to the wire mesh in enhancing the flame stabilization near the blowout limits. The numerical results show that the direction of the thermal path plays a significant role in improving the blowout limits. It is also demonstrated that more heat can be recirculated to the unburned gas region with the use material with higher wall thermal conductivity in burned gas region. As a result, the flame stabilization limits can be enhanced.**

***Index Term*— Micro scale combustion, flame stabilization limits, three-dimensional numerical model**

## INTRODUCTION

The renewed interest in micro power generation is mainly driven by the scarcity of energy resources and the critical need of alternative power sources to batteries. The latest invented electronics devices in the commercial market require greater energy capacity, shorter charging period and lightweight design, characteristics that the conventional batteries lack. Micro power generation systems can be considered as the reliable alternative to the batteries mainly due to high energy density of hydrocarbon fuels [1].

Apart from the energy conversion module, the micro combustor is also the key components in micro power generation system. In order to design a reliable micro power generator, it is essential to understand the underlying combustion fundamentals [2]. Stabilizing flame in narrow channel combustors have been successfully demonstrated [3]. Nonetheless, sustaining stable flame in a micro combustor become a great challenge to researchers. This difficulty is mainly contributed from the high surface to volume ratio of the narrow channel combustors that significantly increase the amount of heat being transferred from the flame to the combustor wall that consequently results to thermal quenching [4] Thus, a proper thermal management is required to ensure that flame can be stabilized inside narrow channel combustors.

Various methods of stabilizing the flame in meso and micro-scale combustors with gaseous fuels have been highlighted. One of the ways of improving the flame stabilization limits of micro burners is by utilizing the principle of excess enthalpy. It was reported that the flame stabilization limits can be enhanced by utilizing a Swiss-roll burner [5]. Nevertheless, the basic fundamentals of determining the flame and flow velocity are still not fully understood mainly due to the complexity of the Swiss-roll geometry and the flame-wall interaction [6]. A simpler combustor geometry is required in order to specifically determine the dependency factors of the flame stabilization. Previous experimental studies pertaining to the utilization of heat recirculation and excess enthalpy principle in tube shape combustors have been reported by several researchers [7,8]. Their results show that by pre-heating the combustor wall in the region of incoming cold reactants, the flame stabilization limits can be improved. Recently, Mikami et al.[9] successfully demonstrated flame stabilization in a meso-scale quartz tube with stainless steel wire mesh for both gas and liquid hydrocarbon fuels. Interestingly, no external heating is required to stabilize the flame. Flame stabilization in narrow channel combustors is influenced by a few factors. Example of these factors are the wall thickness, tube length, and material of the combustor [10]. Few papers have discussed the effect of wall thermal conductivity in narrow channel combustors with gaseous fuels. Kaisare et al. [11] reported that the flame stabilization mechanism in a micro combustor is mainly by upstream heat transfer through the walls. Norton and Vlachos [12] discussed the effect of wall thermal conductivity for a narrow channel combustor with propane-air mixture as the fuel source. However, their discussion is limited to planar combustors without a flame holder. This research investigated factors affecting flame stabilization limits in meso-scale tube combustors with stainless steel wire mesh. Flame stabilization limits in this case is defined as limits in which the flame stabilizes near the wire mesh of the tube combustor. Beyond these limits, two phenomena exist, namely blowout and extinction. Blowout occurs when the flame propagates towards the tube end with an increase of the flow velocity *(U)*. Extinction is a condition where the flame ceases to exist with the decrease of *U*. Both experiments and numerical simulations with three-dimensional (3-D) model were employed to investigate the effect of the wire mesh and the combustor wall thermal conductivity on the flame stabilization. A two-dimensional (2-D) numerical model is not suitable as the conductive heat transfer from the center of the wire mesh to the outer wall of the combustor could not be well represented [13]. The main purpose of the 3-D simulation is to examine important parameters that are difficult to be experimentally obtained.

## I. RESEARCH APPROACH

### A. Experimental Setup

In this experiment, meso-scale combustors made of straight cylindrical tubes were used. Each type of combustor was made of two-piece tubes. A stainless-steel wire mesh was placed in between the two-piece tube dividing between the upstream and the downstream area. The mesh type was 60 mesh/in with wire diameter of 0.14 mm. A heat resistant ceramic adhesive (Ceramabond 569, Aremco Product Inc.) was used to adhere the parts together. The inner diameter of the tube was 3.5 mm with wall thickness of 0.7 mm. The length from the mesh to the upstream part of the tube is defined as the unburned gas region length $L_u$ and $L_b$ is named as the burned gas region length, which is the length between the mesh to the downstream part of the tube. The ambient temperature was set to 295 K, which was maintained at 100 mm horizontally away from the combustor wall. Propane ($C_3H_8$) and air were mixed and supplied into the combustor with an equivalence ratio of $\phi$ and a corresponding cross-sectional-area mean flow velocity of *U*. A mass flow controller (SEC-E440J, HORIBASTEC) was utilized to precisely control the flow rate of the air and fuel. The flame inside the combustor was ignited done by introducing a spark at the exhaust outlet. Once ignited, the flame propagated to the upstream and flame stabilization limits were recorded. For this experiment, a stable flame is defined as a flame that stabilizes near the wire mesh. All combustors have the same unburned gas region length $L_u$, which is 30 mm. This length is adequate for the flow to be fully developed. In addition to that, since the combustor is connected to a copper tube (fuel supply line), it is important to have a reasonable length from the mesh to the connecting point. If the distance is too short, the heat from the wire mesh might be conducted via the combustor wall all the way to the copper tube. This leads to the undesirable effects of reactants being preheated before flowing into the combustor. Consequently, the generated results might be inaccurate. The value of $L_b$ for all combustors is maintained to be at 10 mm. This value is appropriate considering the practical geometry of a meso-scale combustor. For hydrocarbon gaseous combustion, there are two options of fuel type namely methane ($CH_4$) and propane ($C_3H_8$). Propane-air mixture is preferred since it gives better flame stabilization limits than the methane-air mixture. Figure 1(a) and 1(b) shows the schematic diagram of the combustor and the photograph of the stabilized flame.

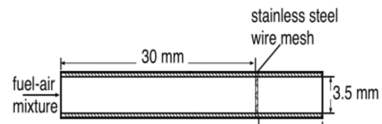


(a)

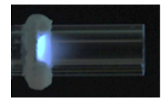

(b)

Fig. 1. Schematic diagram of the tube combustor with wire mesh (b) photography of the stabilized flame.

### B. Numerical Simulation

For the simulation part, a three-dimensional (3-D) steady-state numerical simulation is proposed. The governing equations are solved using ANSYS Academic Release 14.0 with Fluent 6.3 [14]. To be able to quantitatively compare the simulation results with the experimental results, the inner diameter of the combustor is fixed to 3.5 mm, while the wall thickness is maintained to 0.7 mm. The total length of the combustor is fixed to 40.2 mm. The tube combustor is divided into two regions of which defined as unburned and the burned gas region, respectively. The region is divided by stainless steel wire mesh. The wire mesh is located at 30 mm from the center of the combustor inlet. The thickness of the wire mesh is set to 0.20 mm. A three-dimensional (3-D) conductive heat transfer is assumed on the wire mesh with the value of wall thermal conductivity *(k)* is set to 20 W/m/K, which represents the typical value of k for stainless steel [15]. A number of square-shaped holes with length of 0.28 mm are created to let the fluid flows from the inlet to the outlet. Propane ($C_3H_8$)-air mixture is selected as the fuel source. The schematic of the computational domain is shown in Fig.2. Since the calculated range of Reynolds number is between 49 to 200, laminar finite-rate is utilized to solve the fluid flow and combustion interaction. The gas density is calculated based on the ideal gas law while the specific heat of all the species is calculated using a piecewise-polynomial fit of temperature. The mixing law and kinetic theory are employed to solve the specific heat and the thermal coefficient of the gas mixture. To reduce the computational time, overall single step propane-air combustion with five species is employed as the combustion chemistry [16]. This single step reaction model is deemed sufficient since the focus of this study is to examine the flame stabilization phenomenon. A variable grid size is utilized where critical areas of computational domain especially in the burned gas region is given high grid concentration. The minimum grid size is 0.01 mm and the total number of elements is 43548 and employed for all cases. Higher number of elements provide no significant numerical advantage as the flame temperature is hardly changed. The governing equations utilized are the typical fluid motion combined with reacting flows [14].

For the mass diffusion in laminar flows, ANSYS Fluent employs the dilute approximation to model the mass diffusion due to the concentration gradients. The boundary treatment at the interface between the fluid and solid wall is assumed to be no-slip boundary type. The heat flux at this interface is

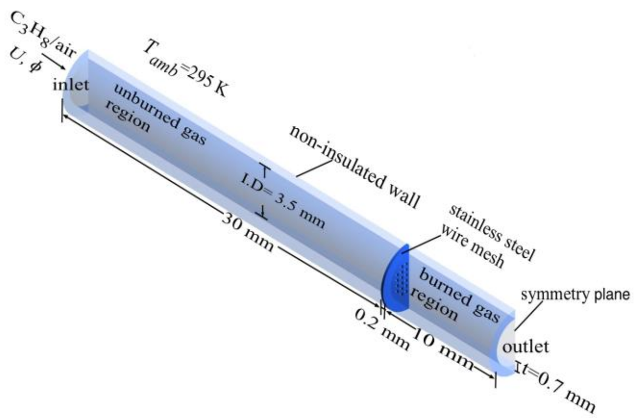


Fig. 2. Computational domain for the 3-D simulation.

calculated using Fourier's law. Heat transfer per unit area by means of convection and radiation at the outer surface of the combustor wall is given as:

$$q_{loss}=h_{conv}\,(T_{wall}-T_{amb})+\varepsilon\sigma(T^4_{wall}-T^4_{amb}) \quad (1)$$

where $h_{conv}$ is the convective heat transfer coefficient, $T_{wall}$ is the wall temperature of the combustor and $T_{amb}$ is defined as the ambient temperature. The value of $T_{amb}$ is initialized to 295 K. The value of $h_{conv}$ is fixed to be at constant 5 W/m$^2$K. The external emissivity (ε) for the outer wall is selected based on the material type of the combustor while value of ε for the wire mesh is set 0.70. The value of Stefan-Boltzmann constant *(σ)* used is $5.67\times10^{-8}\ W/m^2K^4$. A thermal insulation (zero heat flux boundary) is applied at both left and right wall edge of the combustor. For the outlet boundary condition, a fixed pressure inlet is applied. A symmetrical boundary condition is established at the origin of z-plane so that the calculation can be performed only in half of the domain. The material thermal properties and the gas transport data are obtained from Fluent internal database [14] and Kutz [15]. The values of thermodynamics properties for solids used in the numerical model are summarized in Table 1.

Table 1: Values of thermodynamic properties for solids used in the model [15]

| Material name | Wall thermal conductivity, $k$ (W/m.K) | Specific heat $C_p$ (J/kg.K) | Density, $\rho$ (kg/m$^3$) | External emissivity |
|---|---|---|---|---|
| Quartz | 1.6 | 800 | 2500 | 0.90 |
| Stainless steel | 20 | 510 | 7900 | 0.70 |
| Brass | 100 | 380 | 8400 | 0.64 |
| Copper | 400 | 380 | 8960 | 0.60 |

Initially, the momentum and continuity equation is solved. Then, the energy and species equations are solved by applying a sufficiently high temperature of 1600 K to the patching zone, which is defined 1 mm from the outlet. Once ignited, the flame propagates to the upstream and eventually stabilizes near the wire mesh. With a fixed equivalence ratio *(ϕ)*, both blowout and extinction limits are obtained by gradually changing the inlet flow velocity *(U)*.

## II. RESULTS AND DISCUSSION

### A. *Effect of wire mesh on flame stabilization*

This sub-section highlights the results obtained from the numerical simulations. The importance of the wire mesh in enhancing flame stabilization limits can be demonstrated using the developed 3-D numerical model. Simulations with different values of flow velocity (U) were performed and vital parameters such as gas and wire mesh temperature were examined. To demonstrate the validity of the 3-D numerical model, numerical simulations with different type of solid material used in the unburned and burned gas region were performed. The material physical properties are adjusted accordingly as in the reference [15] while the value of the wall thermal conductivity for quartz, brass, and copper is set to be 1.6 W/m/K, 100 W/m/K and 400 W/m/K, respectively. To be easily identified, the name of these combustors is based on the combination of the tube types in both the unburned and the burned gas region. For instance, if a brass tube is utilized in the unburned gas region while a quartz tube is used in the burned gas region, the combustor is named as brass-quartz tube combustor. The similar identification is applied for the rest of the tube combustors.

The results in Fig.3 show that the blowout limits obtained from the simulations are generally higher than the experimental. The highest relative error is recorded for the blowout limits of the brass-quartz tube combustor with 19 % as depicted in Table 2. The main reason for such tendency to occur is due to the utilization of the single step combustion chemistry, which has over-predicted the flame temperature.

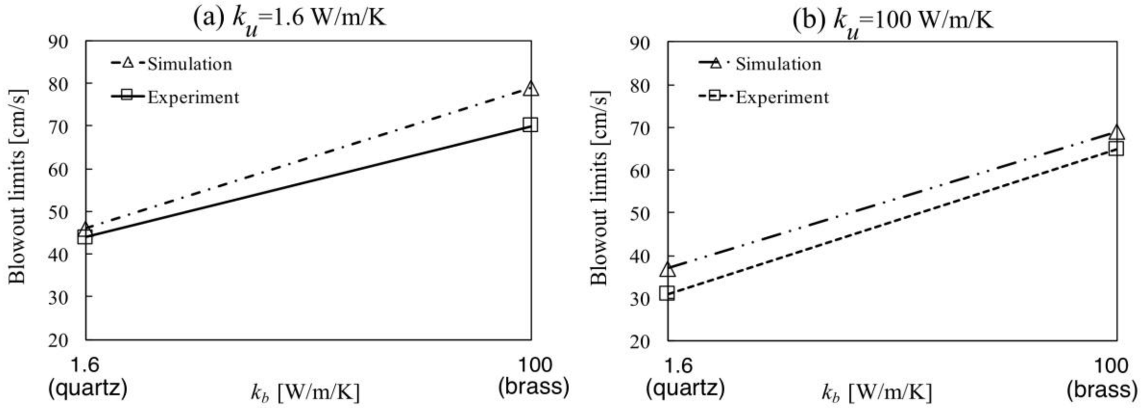


Fig. 3. Blowout limits with different values of $k_b$ for $\phi$=1.0

Meanwhile, Fig.4(a) shows the gas temperature contours while Fig.4(b) presents the wire mesh temperature contours that are taken at different flow velocities (*U*). The value of *U*=10 cm/s is selected since the flame is in a near extinction condition. On the other hand, at *U*=30 cm/s, the flame has been slightly displaced away from the wire mesh, but can still be considered as a stabilized condition. Fig. 4(a) shows that between *U*=10 cm/s to *U*=30 cm/s, there is a difference of 500 K in terms of the flame temperature. With a higher flow velocity, the reaction rate becomes larger, which consequently rises the temperature. It is important to note that the flame temperature is slightly over-predicted due to the use of one-step global combustion chemistry. Meanwhile, Fig. 4(b) suggests that the heat flow direction changes with the variation of U. The alternative term to this heat flow is the thermal path. At *U*=10 cm/s, due to the temperature difference, the heat flows from the wire mesh center towards the combustor outer wall. On the contrary, at *U*=30 cm/s, the heat flows from the wall to the center of the wire mesh.

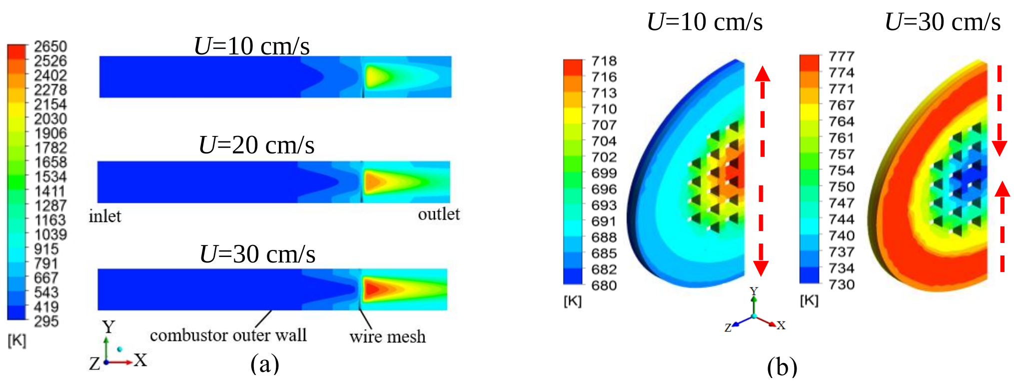


Fig. 4 (a)Gas temperature contours with different flow velocities (*U*) for $\phi$=1.0 for quartz-quartz tube combustor (taken at plane Z=0.28 mm) (b) Wire mesh temperature contours with different flow velocities (*U*) for $\phi$=1.0 for quartz-quartz tube combustor (the arrows indicate the thermal path direction).

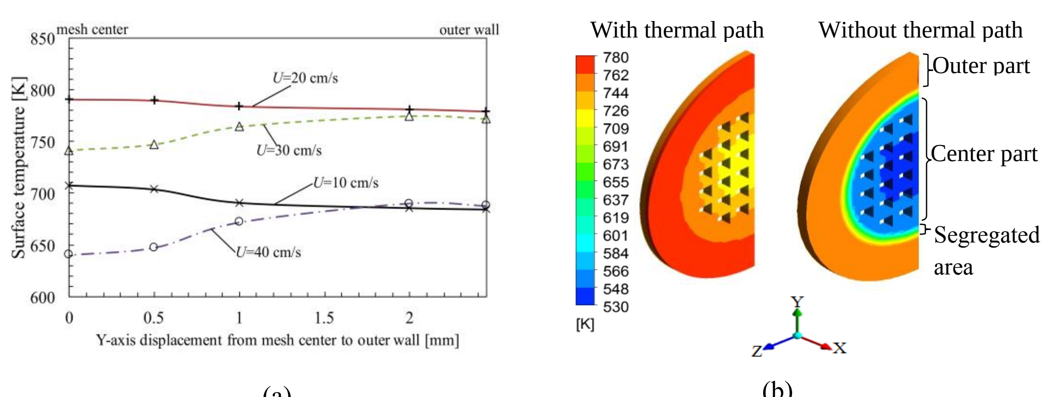


Fig. 5(a) Wire mesh surface temperature with different flow velocities for quartz-quartz tube combustor (line coordinates (X=30.2 mm, Z=0 mm)) (b) Wire mesh temperature contours with and without thermal path for *U*=32 cm/s and $\phi$=1.0 for quartz-quartz tube combustor.

To corroborate the findings in Fig. 4, the numerical values of the wire mesh surface temperature with a wider range of flow velocities are plotted on the same graph as depicted in Fig. 5(a). As shown in the figure, at $U$=10 cm/s and $U$=20 cm/s, the temperature at the center of the wire mesh is higher than the outer wall. Consequently, the transfer of heat from the hot burned gas region to the ambient air via the wire mesh is intensified. A further reduction of $U$ could potentially lead to flame extinction. On the other hand, as the value of $U$ is increased to 30 cm/s and 40 cm/s respectively, the opposite trend occurs. A sufficiently high inlet flow velocity causes the stable flame to be slightly displaced away from the wire mesh. For instance, at $U$=30 cm/s, the flame is located at 0.5 mm from the wire mesh. As a result, the direct transfer of heat from the flame to the wire mesh is reduced. In this condition, the combustor inner wall plays an effective role in recirculating the heat from the burned gas to the unburned gas region via the wire mesh, which subsequently enhances the blowout limits.

The effect of the heat flow or better known as the thermal path between the wire mesh and the combustor inner wall on the flame stabilization is also investigated. A segregated area with a thickness of 0.20 mm is created between the combustor inner wall and the center part of the wire mesh as presented in Fig.5(b). This area is declared as a solid with low wall thermal conductivity. The value of thermal conductivity ($k$) is assigned as 0.0454 W/m/K, which is equivalent to the thermal conductivity of propane-air mixture. By having such isolated area, the effect of the thermal path can be minimized or neglected. Therefore, much of the heat from the burned gas region could not be conducted through the wire mesh to the unburned gas region at high flow velocities. Obviously, this condition could not be performed experimentally. The combustor is assumed to be made of quartz tube for both of the unburned and burned gas region. The blowout limits with this new condition for equivalence ratio ($\phi$) of 1 is then numerically determined. With a disconnected thermal path, the limit is significantly reduced from 46 cm/s to 33 cm/s.

The reduction of almost 28% of the blowout limit is mainly due to the decrease of the surface temperature around the center part of the wire mesh as depicted in Fig.5 (b). As seen in the figure, for the case without the thermal path, there is a temperature different of 130 K between the center and the outer part of the wire mesh. Clearly, without the thermal path, the heat from the burned gas region could not be efficiently recirculated to the wire mesh center. As a result, the temperature around the center part where the unburned gas passes through decreases. Consequently, the blowout limit is significantly reduced.

### *B. Effect of combustor solid material on flame stabilization*

Three types of combustors were fabricated. These combustors utilize different types of solid material in the unburned gas region, namely quartz, brass and copper tube while the tube type used in the burned gas region is fixed to quartz. The dimension of the combustor wall thickness, the length, and the inner wall diameter is maintained as shown in Fig. 1(a).

Experiments were performed to obtain the flame stabilization limits for each of combustor. In a narrow single channel combustor, the axial heat transfer through the combustor wall is considered as the primary mechanism of flame stabilization. Heat is recirculated from the hot burned gas to the unburned gas region, which enables the incoming reactants to be preheated and the flame stabilization limits can be significantly improved. Thus, using a tube with high wall thermal conductivity in the unburned gas region should have resulted in better flame stabilization limits. However, the results show the otherwise. The quartz-quartz tube combustor has the widest flame stabilization limits despite having the lowest wall thermal conductivity. The blowout limits for the quartz-quartz, brass-quartz and copper-quartz tube combustor are 47 cm/s, 35 cm/s and 36 cm/s respectively. All these limits correspond to a slightly rich ($\phi$>1.0) fuel-air mixture.

Since the wire mesh plays a vital role in transferring the heat from the hot burned gas to the unburned gas region, the area-weighted average surface temperature of the wire mesh for all tube combustors is extracted and presented in Fig.6(a). The term $k_u$ is defined as the wall thermal conductivity in the unburned gas region and $k_b$ is assigned as the wall thermal conductivity in the burned gas region. This calculated average temperature is taken around the center of the wire mesh where the fuel-air mixture passes through. It can be deduced from Fig.6(a) that an increase of $k_b$ value leads to a higher wire mesh temperature. However, there is an inverse relationship between the values of $k_u$ and the wire mesh temperature. As seen in Fig.6 (a), the highest wire mesh surface temperature of 883 K is recorded for the quartz-copper tube combustor. On the other hand, the lowest temperature of 465 K is obtained for the copper-quartz tube combustor.

Meanwhile, the blowout limits are depicted in Fig.6(b), which suggest that there is a direct relationship between the value of $k_b$ and the blowout limit. The highest blowout limit of 81 cm/s is obtained for the quartz-copper tube combustor. It can be deduced that the variation of the wire mesh surface temperature directly affects the blowout limits. This dependency is related to the unburned gas temperature, which influences the flame burning velocity. A higher unburned gas temperature leads to an increase of the flame burning velocity. As a result, the blowout limit is also elevated.

Another important parameter for macro and micro tube combustors is the outer wall temperature. Generally, a tube combustor with a uniform outer wall temperature distribution is desired since large temperature gradients can significantly reduce the material lifespan. Fig. 7 shows the outer wall temperature distribution from the inlet to the outlet for a few selected tube combustors. Clearly, the copper-copper tube combustor has the most uniform outer wall temperature distribution with the difference between the hottest and the coolest point is only 39 K.

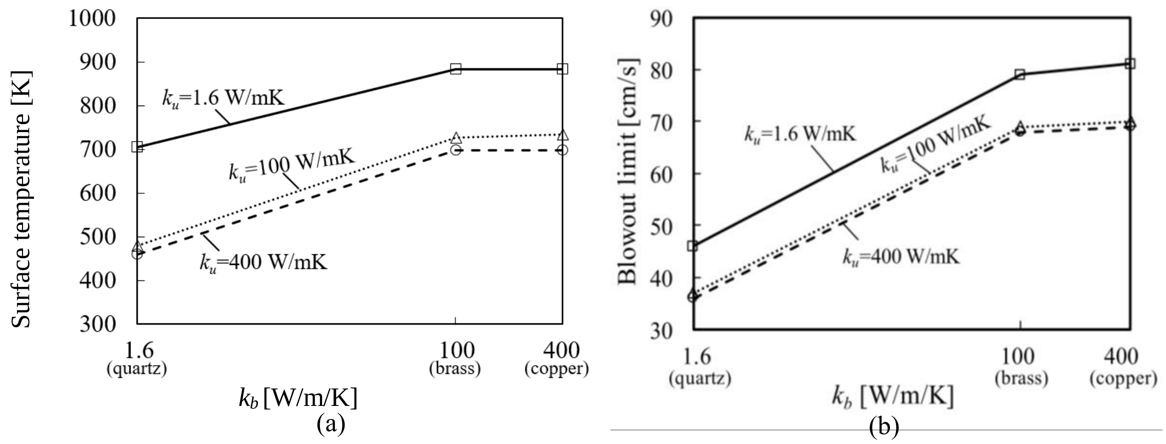


Fig. 6(a) Area-weighted average surface temperature of the wire mesh with different values of $k_b$ for $U$=35 cm/s and $\phi$=1.0 (b) Blowout limits with different values of $k_b$ for $\phi$=1.0.

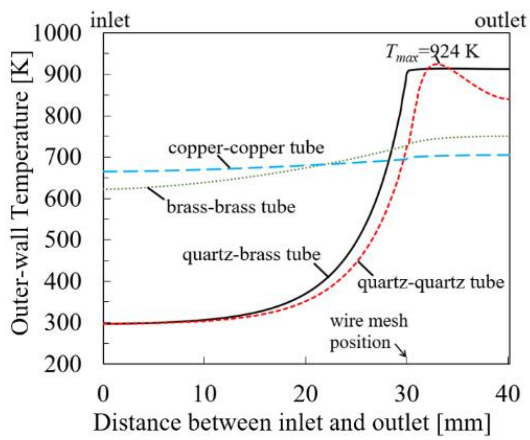


Fig. 7. Outer wall temperature distribution with different types of tube combustors for U=35 cm/s and ϕ=1.0 (line coordinates (Y=0 mm, Z=2.45 mm).

### C. Optimization of the flame stabilization limits

Based on the results obtained from the experiments and numerical simulations that are presented in Section 3.2, the flame stabilization limits of the tube combustors can be further enhanced. The numerical results suggest that the use of solid material with a high wall thermal conductivity in the burned gas region can significantly improve the blowout limits. Therefore, experiments were performed using the combination of quartz and brass tubes with the aim of achieving wider operational limits. The brass tube is selected owing to the cost advantage over the copper tube. Fig.8 depicts the flame stabilization limits with the different types of tube combustors. As indicated in the figure, there is a great improvement of the flame stabilizations limits with the use of quartz-brass combustor. The highest flow velocity before the stable flame is blown out of the tube is 72 cm/s.

Since a uniform and relatively a high outer wall temperature distribution is required for a good tube combustor [10], the quartz tube in the unburned gas region was replaced with a brass tube. Experiments were then conducted to establish the flame stabilization limits for the brass-brass tube combustor and the results are plotted on the same graph as depicted in Fig.8. A slight reduction of the maximum flow velocity from 72 cm/s to 69 cm/s is obtained for the brass-brass tube combustor. Considering the benefit of having a uniform outer wall surface temperature distribution, this reduction is acceptable.

Meanwhile, the combustion efficiency for the quartz-quartz tube and the brass-brass tube combustor is numerically determined and the results are shown in Fig.9. Due to the differences in the values of extinction and blowout limits for each of combustor, the combustion efficiency could not be calculated for certain flow velocities (U). The results indicate that the combustion efficiency for the quartz-quartz tube combustor is higher than the brass-brass tube combustor at all values of U. Nevertheless, the maximum difference in terms of the combustion efficiency between the quartz-quartz and brass-brass tube combustor is only 2.5 %, which occurs at U=2 cm/s.

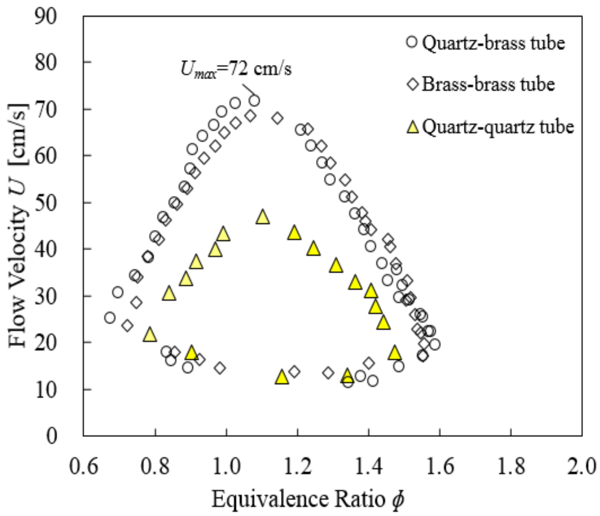


Fig. 8. Flame stabilization limits with different types of combustors.

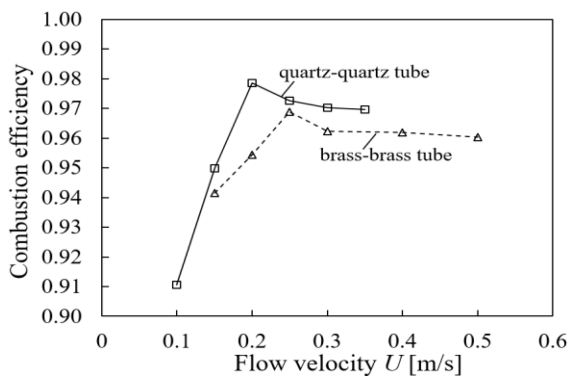


Fig. 9. Combustion efficiency with different flow velocities for the quartz-quartz and the brass-brass tube combustor for ϕ=0.95.

## III. CONCLUSION

A study of flame stabilization in meso-scale tube combustors with wire mesh was successfully conducted. Both experiments and numerical simulations were utilized as the research approach. With the use of three-dimensional (3-D) numerical model, the effective role of the thermal path from the tube combustor wall to the wire mesh in enhancing the flame stabilization limits near the blowout limit was demonstrated.

For the tube combustors with wire mesh, a significant increase of the blowout limits can be obtained with the utilization of a higher wall thermal conductivity in the burned gas region *($k_b$)*. On the contrary, there is an inverse relationship between the wall thermal conductivity in the unburned gas region *($k_u$)* and these limits. This pattern occurs mainly due to the variation of the wire mesh surface temperature where the unburned gas passes through.

Apart from that, the numerical results show that the combustion efficiency for the quartz-quartz tube combustor is higher than the brass-brass tube combustor. Nevertheless, taking into the consideration of the material lifespan and the flame stabilization limits, the brass-brass tube combustor is preferred.

In summary, the results obtained in the experiments and simulations allow for the optimization of flame stabilization in meso-scale tube combustors with wire mesh. This vital knowledge can be further applied to design a reliable combustor, which is the most important component in the micro power generation system.

## REFERENCES

[1] Ju,Y. Maruta, K., Microscale combustion: Technology development and fundamental research, Progress in Energy and Combustion Science, 37 (2011), pp. 669-715.
[2] Raimondeau S., et al., Modeling of high temperature microburners, Proceeding of Combustion Institute, 29 (2002), pp. 901-907.
[3] Miesse, C.M., et al., Submillimeter-scale combustion, AIChE Journal, 50 (2004), pp. 3206-3214.
[4] Wan J., et al., Effect of the length of a plate flame holder on flame blowout limit in a micro-combustor with preheating channels, Combustion and Flame, 170 (2016), pp. 53-62.
[5] Zuo, W., et al., Numerical investigations on thermal performance of a micro-cylindrical combustor with gradually reduced wall thickness, Applied Thermal Engineering, 113 (2010), pp. 1011-1020.
[6] Ju, Y., Xu B., Theoretical and experimental studies on mesoscale flame propagation and extinction, Proceeding of Combustion Institute, 30 (2005), pp. 2445-2453.
[7] Li, J., et al., Effects of heat recirculation on combustion characteristics of n-heptane in micro combustors, Applied Thermal Engineering, 109 (2016), pp. 697-708.
[8] Maruta K., et al., Characteristics of combustion in a narrow channel with a temperature gradient, Proceeding of Combustion Institute, 30 (2005), pp. 2429-2436.
[9] Mikami M., et al., Combustion of gaseous and liquid fuels in meso-scale tubes with wire mesh, Proceeding of Combustion Institute, 34 (2013), pp. 3387-3394.
[10] Shimokuri, D., et al., Effects of inert gases on the vortex bursting in small diameter tubes, Proceeding of Combustion Institute, 34 (2013), 2, pp. 3403-3410.
[11] Kaisare, N.S., Vlachos, D.G., A review on micro combustion: Fundamentals, devices and applications, Progress in Energy and Combustion Science, 38 (2012), pp. 321-359.
[12] Norton, D.G., Vlachos, D.G., A CFD study of propane/air micro flame stability, Combustion and Flame, 138 (2004), pp. 97-107.
[13] Munir, F.A., Mikami M., A numerical study of propane-air combustion in meso-scale tube combustors with concentric rings, Journal of Thermal Science and Technology, 10 (2015), 1, pp. 1-12
[14] ANSYS® Academic Research, Release 14.0, ANSYS FLUENT Tutorial Guide, ANSYS, Inc, 2012.
[15] Kutz, M., Mechanical Engineers Handbook, John Wiley & Sons, New York, USA, 1998.
[16] Westbrook, C.K., Dryer, F.L., Simplified Reaction Mechanism for the Oxidation of Hydrocarbon Fuels in Flames, Combustion Science and Technology, 27 (1981), pp. 31-43.